

# Search for MeV Gamma-ray emission from TeV bright red dwarfs with COMPTEL

Niharika Shrivastava,<sup>1,\*</sup> Siddhant Manna,<sup>2,†</sup> and Shantanu Desai<sup>2,‡</sup>

<sup>1</sup>*Department of Physics, Indian Institute Of Science Education and Research, Bhopal, Madhya Pradesh, 462066, India*

<sup>2</sup>*Department of Physics, IIT Hyderabad, Kandi, Telangana 502284, India*

The SHALON atmospheric Cherenkov telescope has detected very high energy gamma-ray emission at TeV energies from eight red dwarfs, namely, V388 Cas, V547 Cas, V780 Tau, V962 Tau, V1589 Cyg, GJ 1078, GJ 3684 and GL 851.1. Consequently, these red dwarfs have been suggested as sources of ultra-high energy cosmic rays. In this work, we search for soft gamma-ray emission from these TeV bright red dwarfs between 0.75-30 MeV using archival data from the COMPTEL gamma-ray imaging telescope, as a follow-up to a similar search for GeV gamma-ray emission using the Fermi-LAT telescope. Although, prima-facie, we detect non-zero photon flux from three red dwarfs with high significance, these signals can be attributed to contamination from nearby sources such as Crab and Cygnus, which are within the angular resolution of COMPTEL, and have been previously detected as very bright point sources at MeV energies. Therefore, we could not detect any statistically significant signal ( $> 3\sigma$ ) from any of these eight red dwarfs from 0.75-30 MeV. We then report the 95% confidence level upper limits on the differential photon flux (at 30 MeV), integral photon flux and integral energy flux for all of the eight red dwarfs. The integral energy flux limits range between  $10^{-11} - 10^{-10}$  ergs/cm<sup>2</sup>/s.

## I. INTRODUCTION

Red dwarfs are one of the smallest stars on the main sequence with masses between  $0.075-0.5 M_{\odot}$  and surface temperatures between 2,500-5,000 K [1]. They are sometimes synonymous with stellar M-dwarfs. These stars frequently emit flares characterized by a power law with index between 1.7 and 2.4 [2], where the energy of each flare is between  $10^{32}$  and  $10^{35}$  ergs [3]. They account for more than 70% of the galactic stars.

Energetic bursts from red dwarfs have been detected throughout the electromagnetic spectrum. The SWIFT-BAT telescope detected a hard X-ray outburst between 15-50 keV from the flaring dwarf DG CVn, with a luminosity of  $1.9 \times 10^{32}$  ergs/sec along with associated optical emission [4]. A coincident radio flare with flux density greater than 100 mJy was also detected with the AMI-LA radio telescope at 15 GHz [5]. However, no associated emission in gamma-rays between 0.1-100 GeV was seen by the Fermi-LAT detector during this flare [6]. Nevertheless, a gamma-ray pulse from another red dwarf, namely TVLM 513-46546 was detected by Fermi-LAT with a power law index of  $2.59 \pm 0.22$  and having the same periodicity as that seen at optical wavelengths [7]. Most recently, very high energy gamma-ray emission between 800 GeV to 20 TeV has been detected from eight red dwarfs by the SHALON atmospheric Cherenkov telescope [8]. For all these reasons, red dwarfs have also been proposed as sources of ultra high energy cosmic rays [9]. Motivated by all these considerations, a search for GeV gamma-rays from these eight red dwarfs was done using 13.6 years of Fermi-LAT in the energy range from 0.2-500 GeV- [10]. Although GeV gamma-ray emission was seen in the vicinity of two red dwarfs, this signal was excluded as emanating from these red dwarfs based on energetic arguments. Consequently, no significant emission associated with any of the eight red dwarfs could be found [10].

In this work, we look for gamma-ray emission at MeV energies using legacy data from the COMPTEL gamma-ray telescope on the COMPTON gamma-ray observatory, using the same methodology as our previous work, where we looked for MeV emission from galaxy clusters [11] (M24 hereafter). This manuscript is structured as follows. We discuss the data analysis in Sect. II and results in Sect. III. We conclude in Sect. IV.

## II. DATA ANALYSIS

The COMPTEL telescope was one of the three detectors onboard the Compton Gamma Ray Observatory (CGRO) launched in April 1991 which took data until June 2000. This telescope had a field of view of about one steradian and was sensitive to gamma-rays between 0.75- 30 MeV. Its energy and angular resolution ranged

---

\*Email:niharikas21@iiserb.ac.in

†Email:ph22resch11006@iith.ac.in

‡Email:shntn05@gmail.com

between 5-8% and  $(1.7 - 4.4)^\circ$ , respectively depending on the photon energy [12]. COMPTEL did about 340 distinct pointings during its nine years of data taking, where each pointing had a field of view radius of around  $30^\circ$  [13]. More details on the observing specifications and performance of COMPTEL can be found in [12]. COMPTEL has detected a large number of astrophysical sources, such as pulsars, AGNs, X-ray binaries, gamma-ray bursts, solar flares,  $^{26}\text{Al}$ , supernova remnants, extragalactic diffuse gamma-ray background, etc [12, 14]. No other telescope has imaged the universe in the aforementioned energy range after the decommissioning of CGRO. We also note that results from the full survey mission have not yet been released and there could be other undiscovered sources in the dataset [13]. Most recently, new software based on the GammaLib and ctools libraries [15] has been developed facilitating seamless analysis of the COMPTEL data [16]. Therefore, this legacy data provides a unique opportunity to probe the uncharted territory of the universe in soft gamma-rays at MeV energies.

We mine this data to look for MeV emission from each of the eight red dwarfs, which have been detected by SHALON at TeV energies and basically follow the same analysis methodology as M24. We carried out a systematic search within a  $30^\circ$  radius surrounding each target cluster utilizing the revamped COMPTEL analysis framework implemented in the ctools software package [16]. Taking this into consideration, we queried all the COMPTEL pointings encompassing all the nine phases of viewing for all the red dwarfs. The COMPTEL observations are divided into so-called viewing periods (vp) of typically 14 days. The number of viewing periods for each red dwarf are listed in Table I. There was one particular viewing period, vp.0426 (phase 04), pointing to the Anticenter, which was unreadable by the software due to corrupt event processing file and is thereby excluded from our analysis. It was within a  $30^\circ$  radius of three of our red dwarfs, namely V780 Tau, V962 Tau and GJ 1078.

Before commencing the COMPTEL data analysis, we first generated a database from the data available in the HEASARC archive using the `comgendb` tool. Subsequently, we employed the `comobsselect` tool to extract the relevant viewing periods for each red dwarf from the COMPTEL database hosted by HEASARC. For a targeted analysis of each energy bin, the `comobsbin` tool was used to bin the COMPTEL observations into 16 logarithmically spaced energy bins from 0.75 to 30 MeV.

Given the multiple viewing periods, we utilized the `comobsadd` tool with 80 bins each in the  $\chi$  and  $\psi$  directions, where  $\chi$  and  $\psi$  represent the Compton scattering directions [16]. This tool amalgamates individual viewing periods into a single event for each energy band, significantly enhancing the speed of the analysis compared to conducting a joint analysis of each viewing period individually. The cumulative effective exposure from all the viewing periods for all the red dwarfs is presented in Table I.

For maximum likelihood analysis on the data, we generated an appropriate model definition file using the `comobsmodel` tool. This file facilitated fitting the background model to the data and enabled us to analyze our red dwarfs using different templates for point and diffuse sources. We employed point source, radial disk (radius =  $0.2^\circ$ ), and radial Gaussian templates ( $\sigma = 0.2^\circ$ ) as outlined in [17].

The spectral analysis was conducted using the `csspec` tool, akin to the methodology used in M24. We again utilized 16 logarithmically spaced energy bins covering the 0.75-30 MeV range. This tool computes the source spectrum by fitting a model within a given set of spectral bins. It also calculates an upper flux limit, which is particularly useful when the source is not significantly detected within a spectral bin. For this analysis, we applied the BINS method, where the spectral model is replaced by a bin function that fits all the data.

To evaluate the significance we calculated the following test statistic [18]:

$$\text{TS} = 2 \ln L(M_s + M_b) - 2 \ln L(M_b), \quad (1)$$

where  $\ln L(M_s + M_b)$  represents the likelihood when both the source model ( $M_s$ ) and the background model ( $M_b$ ) are fitted to the data. According to Wilks' theorem, TS follows a  $\chi^2$  distribution with  $n$  degrees of freedom, where  $n$  is equal to the number of free parameters for the source model [19]. This same statistics is also used in analysis of data from Fermi-LAT and IceCube [20–22]. In case of null detection, we presented the upper limits for the differential photon flux using a reference energy of 30 MeV, similar to M24.

### III. RESULTS

Our results for the TS values for all the eight red dwarfs can be found in Table I. The reported TS values are the mean values of the TS across all the 16 energy bins. The TS for each energy bin was calculated using the `csspec` tool which we used to make the Spectral Energy Diagrams.

The SED plots for the same are shown in Fig. 1–9. For V388 Cas we find one bin with non-zero flux at energies of 13.39 MeV (cf. Fig 1) with significance of  $0.59\sigma$  with a TS value of 1.4, using a point source template. Similarly, for V547 Cas, we find one bin with non-zero flux at energies of 1.06 MeV (cf. Fig 2) with significance of  $1.74\sigma$  with a TS value of 3.1 using the point source template. Since the significance is less than  $3\sigma$  and detected in only energy bin, we consider this a statistical fluctuation and not a real signal. For GJ 3684 and GL 851.1, we report null detections at all energies.

For the remaining two other red dwarfs namely, V780 Tau and V962 Tau, we detect non-zero flux at the lowest energies from 0.75- 1 MeV with very high significance, and upper limits beyond that with all the three search templates. Similarly, GJ 1078 shows a statistically significant flux at all energies. However, these sources are within  $(3 - 4)^\circ$  of the Crab pulsar (cf. Table I). The angular resolution of COMPTEL gets degraded at low energies making it susceptible to contamination from nearby sources within  $4^\circ$  at very low energies (Jürgen Knödlseher, private communication). Among these sources, GJ 1078 is within  $0.64^\circ$  of the Crab pulsar, which is less than the COMPTEL PSF at all energies [12]. Crab is the brightest source detected in MeV gamma-rays, whose flux between 0.75-1 MeV is equal to  $(16.6 \pm 3.0) \times 10^{-5}$  photons  $\text{cm}^{-2} \text{s}^{-1}$ , between 1-10 MeV it is equal to  $(3.86 \pm 2.12) \times 10^{-5}$  photons  $\text{cm}^{-2} \text{s}^{-1}$ , and between 10-30 MeV it is  $(15.5 \pm 0.5) \times 10^{-5}$  photons  $\text{cm}^{-2} \text{s}^{-1}$  [14]. Therefore, in order to circumvent this issue, for the three aforementioned red dwarfs, we used a template consisting of two sources: one for the Crab pulsar and the other for the red dwarf. Using this two-point source template, we do not detect any signal at these energies, and the SED plots display only upper limits at all energies. The SED plots with both the single and two=point source templates can be found in Fig. 6, Fig. 7, and Fig. 8. We find a similar scenario for these red dwarfs when using a single radial disk or radial Gaussian template and then doing a analysis with two radial disk or radial Gaussian templates. Therefore the statistically significant flux for these three red dwarfs is due to contamination from the nearby Crab pulsar, and cannot be attributed to these red dwarfs.

Similarly, for V1589 Cyg, we see a significant flux from 0.75-1.2 MeV (cf. Fig. 9). However, V1589 Cyg is within  $3.7^\circ$  of Cygnus X-1, whose flux between 0.75-5 MeV is equal to  $(9.78 \pm 0.92) \times 10^{-5}$  photons  $\text{cm}^{-2} \text{s}^{-1}$  [14]. Therefore, we again considered a template of two point sources: one for V1589 Cyg and another for Cygnus. With this change, once again we get only null detections at all energies and the SED plots display upper limits at all energies.

Therefore, we conclude that none of the eight TeV bright red dwarfs show non-zero flux in any energy bin between 0.75-30 MeV with significance  $> 3\sigma$ . We then calculate the 95% confidence level upper limits for the differential photon flux (at 30 MeV), integral photon flux (from 0.75-30 MeV), and the integral energy flux. These upper limits for all the three templates (along with two point source templates for the red dwarfs close to Crab and Cygnus) can be found in Table II. The differential photon flux limits vary between  $10^{-8} - 10^{-7}$  ph/cm<sup>2</sup>/s/MeV, whereas the integral photon flux limits range between  $10^{-6} - 10^{-4}$  ph/cm<sup>2</sup>/s. The integral energy flux limits range between  $10^{-11}$  and  $10^{-10}$  erg/cm<sup>2</sup>/s.

TABLE I: TS values for the Red Dwarfs for each of the red dwarfs using three different search templates, along with total exposure time, number of viewing periods and angular separation to the nearest source (within  $4^\circ$ ) from the first COMPTEL source catalog [14].

Name of Red Dwarf	Template	TS Value	Closest COMPTEL source within $4^\circ$	Angular separation (deg)	Number Of Viewing Periods	Exposure ( $\text{cm}^2\text{s}$ )
V388 Cas	Point Source	0.12	-	-	10	$3.09 \times 10^{10}$
	Radial Disk	0.12				
	Radial Gaussian	0.12				
V547 Cas	Point Source	0.2	-	-	10	$3.09 \times 10^{10}$
	Radial Disk	0.2				
	Radial Gaussian	0.2				
GJ 3684	Point Source	$9.49 \times 10^{-3}$	-	-	13	$3.66 \times 10^{10}$
	Radial Disk	$9.34 \times 10^{-3}$				
	Radial Gaussian	$9.29 \times 10^{-3}$				
GL 851.1	Point Source	$2.93 \times 10^{-2}$	-	-	27	$6.47 \times 10^{10}$
	Radial Disk	$2.96 \times 10^{-2}$				
	Radial Gaussian	$2.97 \times 10^{-2}$				
V780 Tau	Point Source	372.3	Crab pulsar	3.08	23	$6.55 \times 10^{10}$
	Radial Disk	372.7				
	Radial Gaussian	373.8				
	Point Source + Crab	0				
	Radial Disk + Crab	0				
	Radial Gaussian + Crab	0				
V962 Tau	Point Source	462.1	Crab Pulsar	2.75	24	$6.82 \times 10^{10}$
	Radial Disk	462.5				
	Radial Gaussian	463.7				
	Point Source + Crab	0				
	Radial Disk + Crab	0				
	Radial Gaussian + Crab	0				
GJ 1078	Point Source	497.2	Crab Pulsar	0.64	23	$6.55 \times 10^{10}$
	Radial Disk	497.6				
	Radial Gaussian	498.5				
	Point Source + Crab	0				
	Radial Disk + Crab	0				
	Radial Gaussian + Crab	0				
V1589 Cyg	Point Source	5.45	Cygnus X-1	3.7	20	$3.88 \times 10^{10}$
	Radial Disk	5.46				
	Radial Gaussian	5.48				
	Point Source + Cygnus	0				
	Radial Disk + Cygnus	0				
	Radial Gaussian + Cygnus	0				

TABLE II: Results for MeV gamma-ray emission from the eight red dwarfs searched using COMPTEL data. We report 95% c.l. upper limits for differential flux (at 30 MeV), integral flux, and energy flux for all the three search templates used along with two source templates for the red dwarfs which reported significant detections at the lowest energies.

Name of Red Dwarf	Template	Differential Flux at 30 MeV (ph/cm <sup>2</sup> /s/MeV)	Integral Photon Flux (ph/cm <sup>2</sup> /s)	Integral Energy Flux (erg/cm <sup>2</sup> /s)
V388 Cas	Point Source	$< 3.57 \times 10^{-7}$	$< 9.83 \times 10^{-5}$	$< 1.75 \times 10^{-10}$
	Radial Disk	$< 3.57 \times 10^{-7}$	$< 9.83 \times 10^{-5}$	$< 1.76 \times 10^{-10}$
	Radial Gaussian	$< 3.56 \times 10^{-7}$	$< 9.85 \times 10^{-5}$	$< 1.76 \times 10^{-10}$
V547 Cas	Point Source	$< 3.32 \times 10^{-7}$	$< 1.14 \times 10^{-4}$	$< 1.35 \times 10^{-10}$
	Radial Disk	$< 3.33 \times 10^{-7}$	$< 1.14 \times 10^{-4}$	$< 1.35 \times 10^{-10}$
	Radial Gaussian	$< 3.34 \times 10^{-7}$	$< 1.14 \times 10^{-4}$	$< 1.36 \times 10^{-10}$
GJ 3684	Point Source	$< 9.31 \times 10^{-7}$	$< 5.73 \times 10^{-5}$	$< 1.77 \times 10^{-10}$
	Radial Disk	$< 9.32 \times 10^{-7}$	$< 5.72 \times 10^{-5}$	$< 1.77 \times 10^{-10}$
	Radial Gaussian	$< 9.36 \times 10^{-7}$	$< 5.73 \times 10^{-5}$	$< 1.77 \times 10^{-10}$
GL 851.1	Point Source	$< 3.34 \times 10^{-7}$	$< 5.54 \times 10^{-5}$	$< 1.52 \times 10^{-10}$
	Radial Disk	$< 3.34 \times 10^{-7}$	$< 5.54 \times 10^{-5}$	$< 1.52 \times 10^{-10}$
	Radial Gaussian	$< 3.35 \times 10^{-7}$	$< 5.56 \times 10^{-5}$	$< 1.53 \times 10^{-10}$
V780 Tau	Point Source + Crab	$< 1.02 \times 10^{-7}$	$< 5.29 \times 10^{-6}$	$< 1.73 \times 10^{-11}$
	Radial Disk + Crab	$< 1.02 \times 10^{-7}$	$< 5.29 \times 10^{-6}$	$< 1.73 \times 10^{-11}$
	Radial Gaussian + Crab	$< 1.02 \times 10^{-7}$	$< 5.30 \times 10^{-6}$	$< 1.73 \times 10^{-11}$
V962 Tau	Point Source + Crab	$< 8.40 \times 10^{-8}$	$< 4.62 \times 10^{-6}$	$< 1.50 \times 10^{-11}$
	Radial Disk + Crab	$< 8.41 \times 10^{-8}$	$< 4.62 \times 10^{-6}$	$< 1.50 \times 10^{-11}$
	Radial Gaussian + Crab	$< 8.43 \times 10^{-8}$	$< 4.63 \times 10^{-6}$	$< 1.50 \times 10^{-11}$
GJ 1078	Point Source + Crab	$< 7.21 \times 10^{-8}$	$< 4.60 \times 10^{-6}$	$< 1.40 \times 10^{-11}$
	Radial Disk + Crab	$< 7.22 \times 10^{-8}$	$< 4.60 \times 10^{-6}$	$< 1.4 \times 10^{-11}$
	Radial Gaussian + Crab	$< 7.23 \times 10^{-8}$	$< 4.62 \times 10^{-6}$	$< 1.40 \times 10^{-11}$
V 1589 Cyg	Point Source + Cygnus	$< 8.64 \times 10^{-8}$	$< 4.86 \times 10^{-6}$	$< 1.62 \times 10^{-11}$
	Radial Disk + Cygnus	$< 8.63 \times 10^{-8}$	$< 4.86 \times 10^{-6}$	$< 1.62 \times 10^{-11}$
	Radial Gaussian + Cygnus	$< 8.63 \times 10^{-8}$	$< 4.86 \times 10^{-6}$	$< 1.62 \times 10^{-11}$

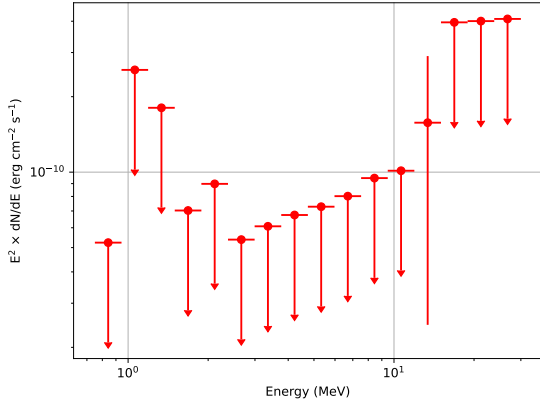


FIG. 1: V388 Cas

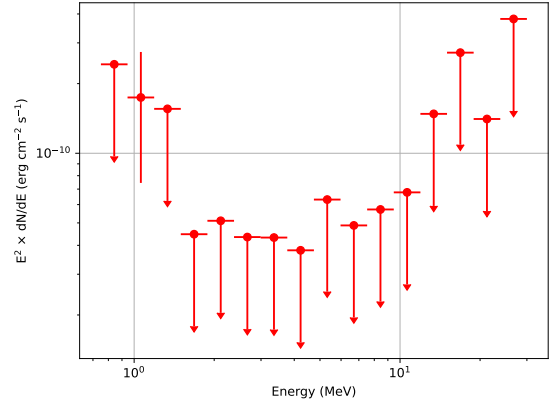


FIG. 2: V780 Cas

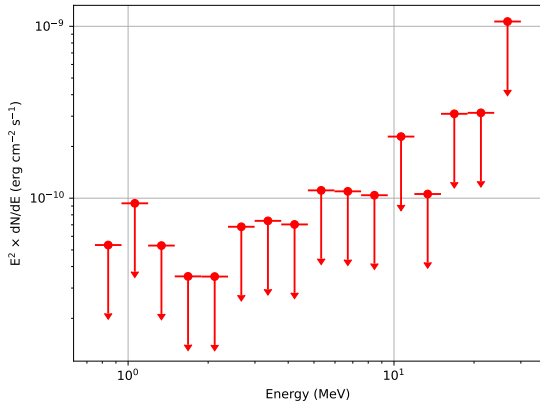


FIG. 3: GJ 3684

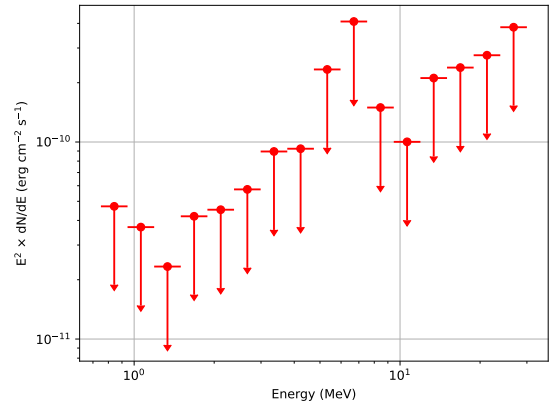
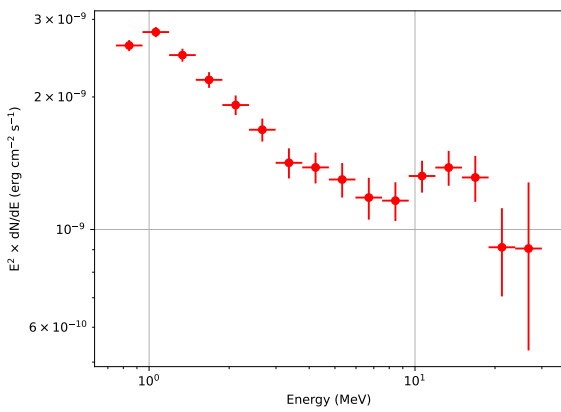
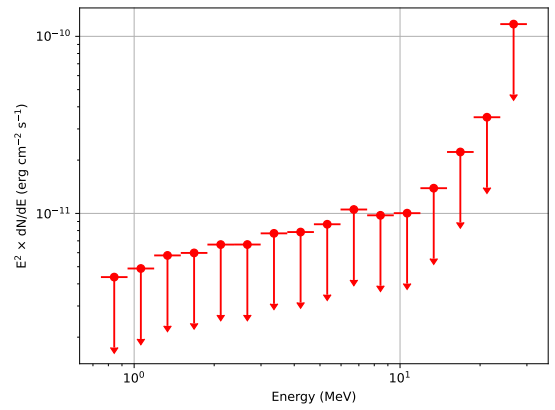


FIG. 4: GL 851.1

FIG. 5: SED plot using single point source analysis of red dwarfs.

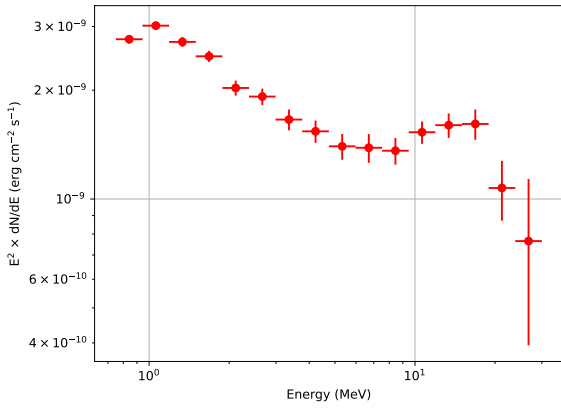


(a) SED using a single point source template

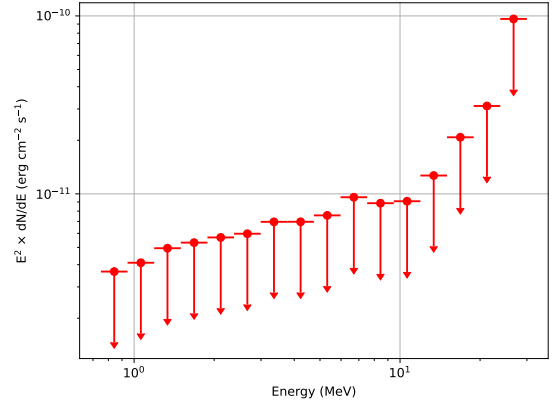


(b) SED using two point source templates including the Crab pulsar.

FIG. 6: One point and two point source analyses plots for V780 Tau.

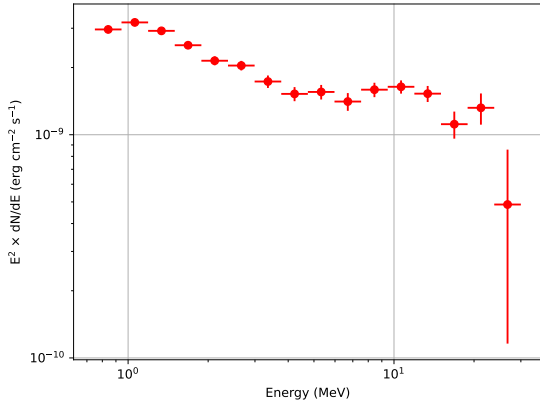


(a) SED using using a single point source template.

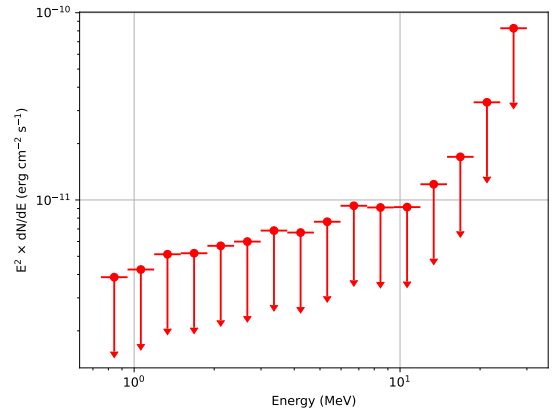


(b) SED using two point source templates including the Crab pulsar.

FIG. 7: One point and two point source analyses plots for V962 Tau.

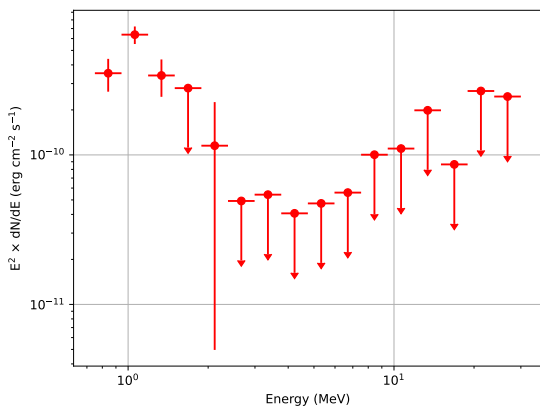


(a) SED using a single point source template.

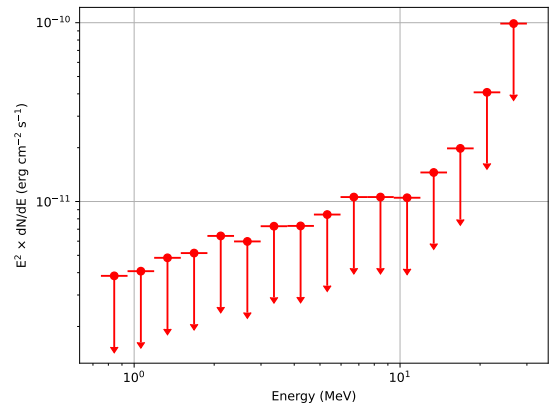


(b) SED using two point source templates including the Crab pulsar.

FIG. 8: One-point and two-point source analyses plots for GJ 1078.



(a) SED using a single point source template.



(b) SED using point source templates including Cygnus.

FIG. 9: One-point and two-point analysis plots for V1589 Cyg

#### IV. CONCLUSIONS

Recently, very high energy gamma-ray emission has been detected from eight red dwarfs between 800 GeV to 20 TeV, namely V388 Cas, V547 Cas, V780 Tau, V962 Tau, V1589 Cyg, GJ 1078, GJ 3684, and GL 851.1 from the SHALON atmospheric Cherenkov telescope [8]. A recent work also looked for GeV gamma-ray emission between 0.2-500 GeV with Fermi-LAT [10]. On the other hand, the soft gamma-ray energy band (between  $\sim 1$ -30 MeV) is uncharted territory and has not been imaged by any other gamma-ray telescope after the decommissioning of the COMPTEL MeV telescope in 2000. About two years ago, new software has been released to facilitate seamless analysis of the archival COMPTEL data [16].

Motivated by all these considerations, we search for soft MeV gamma-ray emission (0.75 - 30 MeV) from these aforementioned eight red dwarfs using archival data from the COMPTEL gamma-ray telescope. For our analysis, we used three search templates: point source, radial disk, and radial Gaussian (similar to our recent work on searching from MeV emission from galaxy clusters [11]).

Three of the above red dwarfs, viz. V780 Tau, V962 Tau, V1589 Cyg, prima-facie show a statistically significant flux below 1 MeV, whereas GJ 1078 shows non-zero flux with high significance at all energies. However, at energies around 1 MeV, the angular resolution of COMPTEL gets degraded to several degrees and the signal could get contaminated by nearby sources. These sources are within the vicinity of Crab pulsar or Cygnus, which have been detected as very bright sources from the first COMPTEL point source catalog. GJ 1078 is within  $0.64^\circ$  of the Crab pulsar and hence is contaminated by the signal from Crab at all energies. Therefore, we also fit for the nearest source along with the red dwarf. Once we do that, we obtain null detections for the aforementioned three red dwarfs at all energies. Two other red dwarfs, GJ 3684 and GL 851.1 also show null detections at all energies. Finally the remaining two red dwarfs (V388 Cas and V547 Cas) report a non-zero flux in only one energy bin at 13.39 MeV and 1.06 MeV, respectively. However the statistical significance of this signal is only  $0.59\sigma$  and  $1.74\sigma$ , respectively and therefore can only be considered as a fluctuation. The SED for all these red dwarfs can be found in Figs. 1 to Figs 9.

Therefore, we do not detect any signal from these red dwarfs at soft MeV energies with significance  $> 3\sigma$  using archival data from the COMPTEL gamma-ray telescope. We then report the 95% c.l. upper limits on the integral and differential photon flux (at 30 MeV), along with integrated energy flux limits. These limits have been collated in Table II. The integral energy flux limits range between  $10^{-11} - 10^{-10}$  ergs/cm<sup>2</sup>/s.

#### Acknowledgments

NS has been supported by a Summer Undergraduate Research Exposure(SURE) Internship at IIT Hyderabad. SM is supported by Government of India, Ministry of Education (MOE) fellowship. We are also very grateful to Jürgen Knödlseeder for once again explaining the nuances of the COMPTEL analysis software and generously helping us with all the doubts faced.

- 
- [1] K. E. Edgeworth, *Nature (London)* **157**, 481 (1946).
  - [2] M. J. Aschwanden and M. Güdel, *Astrophys. J.* **910**, 41 (2021), 2106.06490.
  - [3] H. Yang, J. Liu, Q. Gao, X. Fang, J. Guo, Y. Zhang, Y. Hou, Y. Wang, and Z. Cao, *Astrophys. J.* **849**, 36 (2017).
  - [4] S. Drake, R. Osten, K. L. Page, J. A. Kennea, S. R. Oates, H. Krimm, and N. Gehrels, *The Astronomer's Telegram* **6121**, 1 (2014).
  - [5] R. P. Fender, G. E. Anderson, R. Osten, T. Staley, C. Rumsey, K. Grainge, and R. D. E. Saunders, *MNRAS* **446**, L66 (2015), 1410.1545.
  - [6] A. Loh, S. Corbel, and G. Dubus, *MNRAS* **467**, 4462 (2017), 1702.03754.
  - [7] Y. Song and T. A. D. Paglione, *Astrophys. J.* **900**, 185 (2020), 2008.01143.
  - [8] V. G. Sinitsyna, V. Y. Sinitsyna, and Y. I. Stozhkov, *Advances in Space Research* **64**, 2585 (2019).
  - [9] V. Y. Sinitsyna, V. G. Sinitsyna, and Y. I. Stozhkov, in *European Physical Journal Web of Conferences* (2022), vol. 260 of *European Physical Journal Web of Conferences*, p. 11033.
  - [10] C. Huang, X. Zhang, Y. Chen, and W. Zhong, *Astrophys. J.* **965**, 26 (2024), 2403.12524.
  - [11] S. Manna and S. Desai, *JCAP* **2024**, 013 (2024), 2401.13240.
  - [12] V. Schoenfelder, H. Aarts, K. Bennett, H. de Boer, J. Clear, W. Collmar, A. Connors, A. Deerenberg, R. Diehl, A. von Dordrecht, et al., *Astrophys. J. Suppl. Ser.* **86**, 657 (1993).
  - [13] A. Strong and W. Collmar, *Memorie della Societa Astronomica Italiana* **90**, 297 (2019), 1907.07454.
  - [14] V. Schönfelder, K. Bennett, J. J. Blom, H. Bloemen, W. Collmar, A. Connors, R. Diehl, W. Hermsen, A. Iyudin, R. M. Kippen, et al., *Astronomy and Astrophysics Supplement Series* **143**, 145 (2000), astro-ph/0002366.
  - [15] J. Knödlseeder, M. Mayer, C. Deil, J. B. Cayrou, E. Owen, N. Kelley-Hoskins, C. C. Lu, R. Buehler, F. Forest, T. Louge, et al., *Astron. & Astrophys.* **593**, A1 (2016), 1606.00393.



- [16] J. Knödseder, W. Collmar, M. Jarry, and M. McConnell, *Astron. & Astrophys.* **665**, A84 (2022), 2207.13404.
- [17] M. Wood, R. Caputo, E. Charles, M. Di Mauro, J. Magill, J. S. Perkins, and Fermi-LAT Collaboration, in *35th International Cosmic Ray Conference (ICRC2017)* (2017), vol. 301 of *International Cosmic Ray Conference*, p. 824, 1707.09551.
- [18] J. R. Mattox, D. L. Bertsch, J. Chiang, B. L. Dingus, S. W. Digel, J. A. Esposito, J. M. Fierro, R. C. Hartman, S. D. Hunter, G. Kanbach, et al., *Astrophys. J.* **461**, 396 (1996).
- [19] S. S. Wilks, *The annals of mathematical statistics* **9**, 60 (1938).
- [20] S. Manna and S. Desai, *JCAP* **2024**, 017 (2024), 2310.07519.
- [21] V. Pasumarti and S. Desai, *JCAP* **2022**, 002 (2022), 2210.12804.
- [22] V. Pasumarti and S. Desai, *JCAP* **2024**, 010 (2024), 2306.03427.